Mechanics and Mechanical Engineering
Vol. 19, No. 1 (2015) 63–75

Element Birth and Death Method Application to Lamellar Crack Analysis

Mieczysław JARONIEK
Department of Strength of Materials
Lodz University of Technology
Stefanowskiego 1/15, 90–924 Łódź, Poland

Tadeusz NIEZGODZIŃSKI
Department of Mechanics and Mechanical Engineering
Higher Vocational State School
3 Maja 17, 87-800 Włocławek, Poland

Received (10 September 2015)
Revised (16 September 2015)
Accepted (27 September 2015)

Load structure, the maximum permissible load is usually determined by the strength calculation (bearing data. Yield stress or strength of the material), or the parameters of fracture mechanics. The paper analyzes the calculations lamellar cracks formed in the lower crane girders steel belts.

These cracks are formed in rolled sheets of non–metallic inclusions. The determination of the cracks in the existing designs are extremely difficult. It requires testing metallographic, ultrasonic or acoustic methods. Based on typical images of metallographic steel plates specified place of occurrence of cracks lamellar and sampling, and has subsequently been adopted for the calculation of numerical models of material structure and distribution of artificial joints. In order to analyze the propagation of cracks and formation of lamellar phase slots and destruction was carried out modeling studies and numerical methods cracking process.

Keywords: FEM, model of fracture, stress intensity–factor, lamellar cracks.

1. Introduction

Metallographic examinations supplemented by numerical calculations and research mock–lamellar cracks allow analysis of their interaction in the pre–destruction and the process of cracking.

In order to determine the course of gaps in critical loads cause cracking of the finite element method to comply with "Element Birth and Death Method". This method consists in the fact that when the apex slots are exceeded the maximum stress or intensity factor stress reaches a critical value, i.e. $K_I = K_{IC}$ then it is

assumed that elements in the top of the gap disappears, the gap is increased, the cycle calculation is repeated again assumed the stress intensity factor, which reaches a critical value, etc.

Since the crack may propagate if the normal stresses surface gaps are extending causing dilation of a gap, it was decided to use the hypothesis Burzynski to designate the reduced stresses. The hypothesis Burzynski is a modification of the hypotheses Huber.

It allows you to take into account the impact of the difference between the tensile strength and compressive strength. This approach allows you to visualize the places which produce the maximum stress reduced with significant influence of a tensile component. Figs 4 and 7 show maps of reduced stresses by hypothesis Burzynski made on the basis of metallographic analysis. The scale of the stress ends with the value of 150 MPa.

2. Numerical methods for determining stress intensity factors $K_I and K_{II}$

Surrounded by the top of the slot components of stresses and displacements in polar coordinates r, φ you can describe the basic formulas given m. Al. in the work [1], [4], [8], [9].

$$\begin{aligned}
\sigma_x &= \frac{K_I}{\sqrt{2\pi r}}\cos\frac{\Theta}{2}\left(1-\sin\frac{\Theta}{2}\sin\frac{3\Theta}{2}\right)+\sigma_{ox}\\
\sigma_y &= \frac{K_I}{\sqrt{2\pi r}}\cos\frac{\Theta}{2}\left(1+\sin\frac{\Theta}{2}\sin\frac{3\Theta}{2}\right)\\
\tau_{xy} &= \frac{1}{\sqrt{2\pi r}}\left[K_I\sin\frac{\Theta}{2}\cos\frac{\Theta}{2}\cos\frac{3\Theta}{2}\right)+K_{II}\cos\frac{\Theta}{2}\left(1-\sin\frac{\Theta}{2}\sin\frac{2\Theta}{2}\right)]\\
\sigma_x &= \frac{K_I}{\sqrt{2\pi r}}\cos\frac{\Theta}{2}\left(1-\sin\frac{\Theta}{2}\sin\frac{3\Theta}{2}\right)+\sigma_{ox} \qquad (1)\\
\upsilon &= \frac{K_I}{4G}\sqrt{\frac{r}{2\pi}}\left[(2\kappa+1)\sin\frac{\Theta}{2}-\sin\frac{3\Theta}{2}\right]\\
&\quad -\frac{K_{II}}{4G}\sqrt{\frac{r}{2\pi}}\left[(2\kappa+3)\cos\frac{\Theta}{2}+\cos\frac{3\Theta}{2}\right]+O(r)\\
w &= \frac{K_I}{4G}\sqrt{\frac{r}{2\pi}}\sin\frac{\Theta}{2}+O(r)
\end{aligned}$$

when: $\kappa = 3-4\nu$ for plain strain and $\kappa = \frac{3-\nu}{1+\nu}$ for plain stress.

These patterns can be used for calculation of stress intensity factors based on numerical calculations for $\Theta = \pm\,\pi$ ($\pm\,180^\circ$):

$$\begin{aligned}
\sigma_x &= \frac{K_I}{\sqrt{2\pi r}}\cos\frac{\Theta}{2}\left(1-\sin\frac{\Theta}{2}\sin\frac{3\Theta}{2}\right)+\sigma_{ox}\\
\upsilon &= \frac{K_I}{2G}\sqrt{\frac{r}{2\pi}}(1+\kappa) \qquad (2)\\
w &= \frac{2K_{III}}{G}\sqrt{\frac{r}{2\pi}}
\end{aligned}$$

given the values of displacements (u, v, w) and the corresponding values of r can calculate stress intensity factors by design:

$$\begin{aligned} \sigma_x &= \frac{K_I}{\sqrt{2\pi r}} \cos\frac{\Theta}{2}(1 - \sin\frac{\Theta}{2}\sin\frac{3\Theta}{2}) + \sigma_{ox} \\ K_{II} &= \sqrt{2\pi}\frac{2G}{1+\kappa} \cdot \frac{|u|}{\sqrt{r}} \\ K_{III} &= \sqrt{2\pi}2G \cdot \frac{|w|}{\sqrt{r}} \end{aligned} \tag{3}$$

For comparison of experimental results with analytical calculations and numerical methods (finite elements method - FEM) calculations were carried out using ANSYS 14.

$$\sigma_y = \frac{K_I}{\sqrt{2\pi r}} \cos\frac{\Theta}{2}(1 + \sin\frac{\Theta}{2}\sin\frac{3\Theta}{2}) \quad \tau_{xy} = \frac{1}{\sqrt{2\pi\, r}} K_{II}$$

from

$$\sigma_x = \frac{K_I}{\sqrt{2\pi r}} \cos\frac{\Theta}{2}(1 - \sin\frac{\Theta}{2}\sin\frac{3\Theta}{2}) + \sigma_{ox} \quad and \quad K_{II} = \tau_{xy}\sqrt{2\pi\, r} \tag{4}$$

Analysis of the cracking process carried out by finite element method is a shared structure in the vicinity of slots for a very large number of small components and the calculation of the stress intensity factors based on displacement nodes at the edges of the slot or under stress in the surrounding tip slot, $\Theta = 0$.

For calculation basically two different divisions of the finite element mesh rectangular grid of 8–node and recommended for the calculation of fracture mechanics parameters triangular mesh 6-node. For each type of mesh used various types of compaction elements about the vertices of the slots. Performing numerical finite element method was to compare the results with those used methods analytical and numerical calculations.

The division of the structure surrounded by the tip slot to a very large number of small elements also has some limitations also lead to similar inaccuracies as singularity around the top slot in the analytical solutions. For a very large number of very small elements in the environment apex slots receive stress exceeding many times the strength of the material, and even critical values of the forces of cohesion. Thus it is in a sense the virtual tension. To illustrate such a situation, numerical calculations were performed for two different networks: Rectangular 8–node and the triangular mesh 6–node for each of these grids was used similar types of compaction elements about the vertices of the slots.

For materials with linear elastic characteristics of the stress-strain we observed following rule. Mathematical description of stress, assuming a singularity at tip of the crack slot at $x \to 0$ $\sigma_y \to \infty$ allows you to specify the size of the stress intensity factors by formulas (1) or (2) as a function of stress in the environment the top of the slot or load, but in terms of linear fracture mechanics at the apex $\sigma_y \to \infty$ slots stress (as well as $\sigma_x \to \infty$ and $\tau_{xy} \to \infty$). The same regularity stress increase as the division of the structure into smaller elements observed by both numerical calculations using finite element programs as well as numerical procedures used to

describe the stress using analytic functions. Nevertheless, even when broken down into very large number of very small components in the calculation of finite element stress have a finite value.

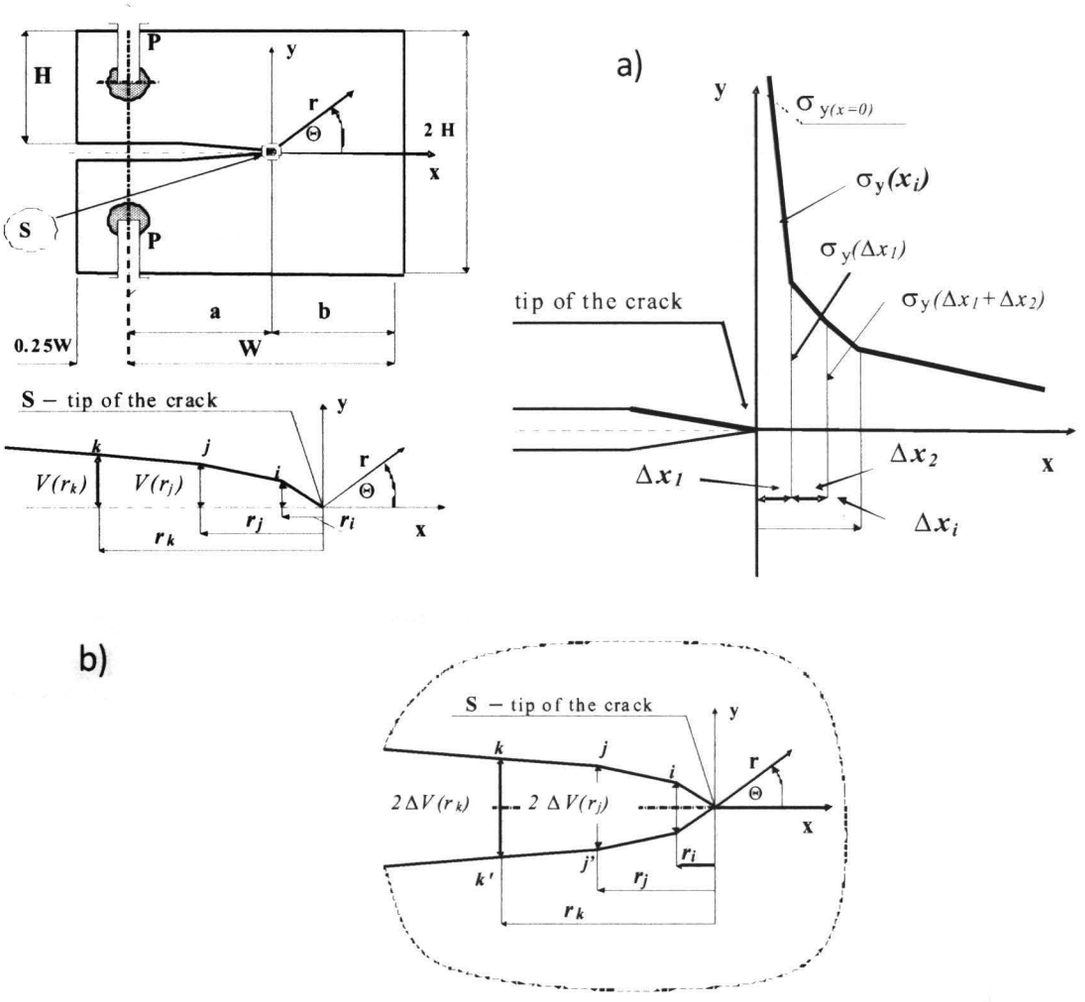

Figure 1 a) Schematic of the sample CT designations used in numerical calculations of stresses, displacements and surrounded the tip of the crack, the stress intensity factors, b) the amount of displacement between points on opposite banks of slots (e.g. K k')

2.1. *Assumptions for calculations*

It was assumed:

– plane strain and affirmation left edge of the structure model – moving the right edge of the model of $\varepsilon_x = 0.06\%$.

Steel structure modeled adopting the following material information:

– Ferrite: elastic material order

Young's modulus in the range of elastic E = 204 GPa

Young's modulus in the range of plastic E_p = 10 GPa

Poisson's ratio $\nu = 0.3$

yield strength R_e = 150 MPa

tensile strength R_m= 300 MPa

– Non–metallic inclusions:
Young's modulus E = 1 MPa
Poisson's ratio $\nu = 0.499$

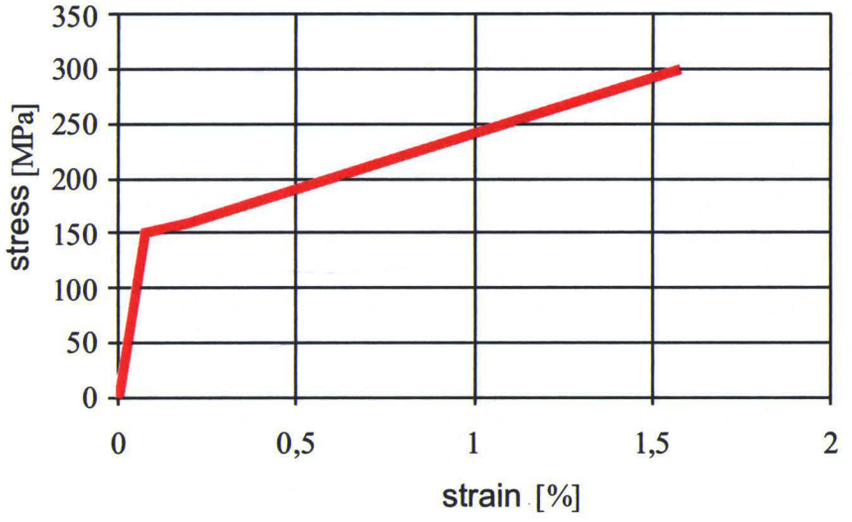

Figure 2 The dependence of the stress-strain to the ferrite

3. Material data

Table 1 Characteristics of (material) structures

	Tensile strength R_m [MPa]	Yield strength R_e [MPa]	Young's modulus E [GPa]	Poisson's ratio ν
Ferryt	330	150	211	0.295
Perlit	620	400	205	0.29
MnS	-	-	70	0.33
Al_2O_3	300	-	370	0.22

During normal operation, the bands crane lower steel girders are loaded with acceptable tensile stress (the bending) of around $\sigma_r = 150$MPa. The accepted steel Young's modulus E = 2 10^5 MPa tensile strain are

It was assumed:

– plane strain and affirmation left edge of the structure model - moving the right edge of the model of $\varepsilon_x = 0.06\%$, $\varepsilon_x = \sigma_r$ / E = 120/2 10^5 = 0.0006 = 0.06%

Steel belts used on the lower girder consists mainly of ferrite. Perlite and non–metallic inclusions are smaller quantity. These deformations cause stress concentrations in non–uniform structure (i.e. pearlite + ferrite).

The calculations were made for the elements of the bottom box girder span L = 28 m. It was assumed that the longitudinal slots (lamellar) cracks occur only in the lower flange of the girder.

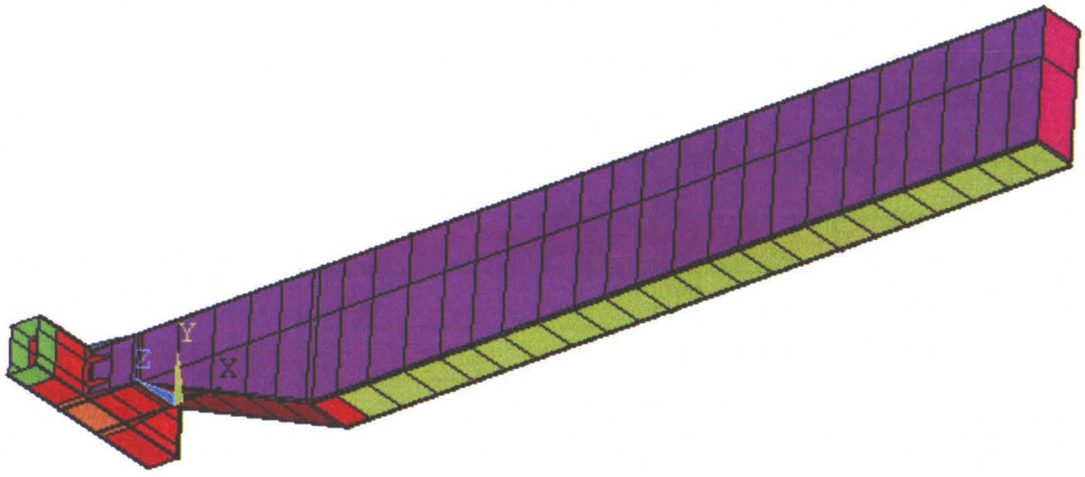

Figure 3 View of the bottom crane with inclusions (green)

The influence of the quantity of breakages on the value of the deflection during operation of such a structure. The model fracture was carried out using a discretization of the bottom element of the multi–layer coating.

For the analysis of stress and strain in part modeling sheet structure used in flat triangular element A six PLANE2.

It was assumed:

– Order right edge model

– Restrain the left edge of the structure model.

Steel belts used on the lower girder consists mainly of ferrite. Perlite and non–metallic inclusions are smaller quantity. These deformations cause stress concentrations in non–uniform structure (i.e. pearlite + ferrite).

The calculations were performed using the finite element program ANSYS 14. For comparison of experimental results with analytical calculations and numerical methods (finite elements method – FEM) was also performed calculations using ANSYS 14 using a special division for 6–node triangular finite elements, like in [6] – e.g. Fig. 6.

For different types of samples was performed to calculate the numerical and analytical data for calculations by adopting the same as in experimental studies.

For the analysis of stress and strain in part modeling sheet structure used in flat triangular element a six PLANE 2. Each node has two degrees of freedom – the ability to move in two mutually perpendicular directions.

Model loaded displacements in the plane strain, which corresponds to the hypothesis of the flat cross sections of the bottom beam during use. Assuming the beginning of the process of cracking occurs in ferrite the following assumptions: Special arrangement of the elements and non homogeneous structure of the material. The small size of the inclusions required to modeled steel structure was the analysis of the micro.

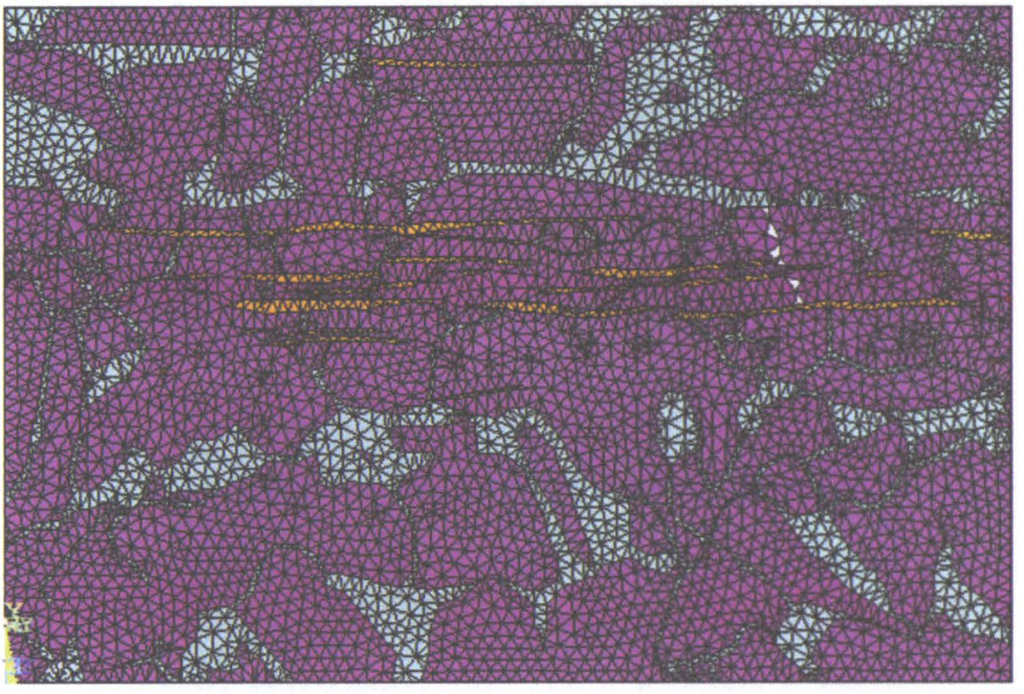

Figure 4 FEM model generated based on metallographic examination

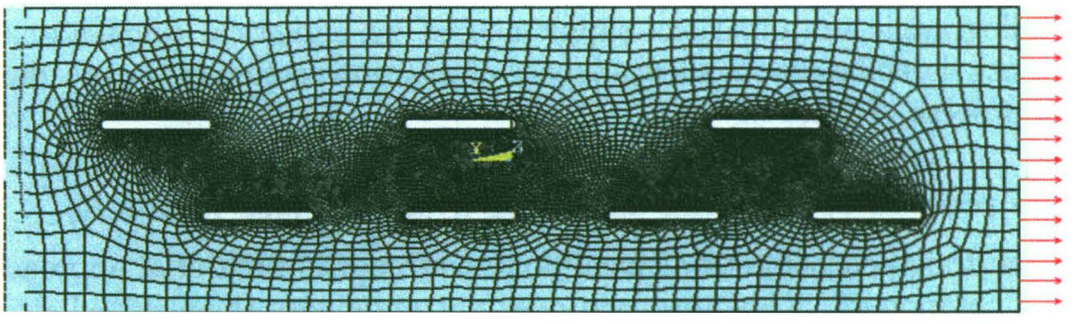

Figure 5 FEM model of sample voids

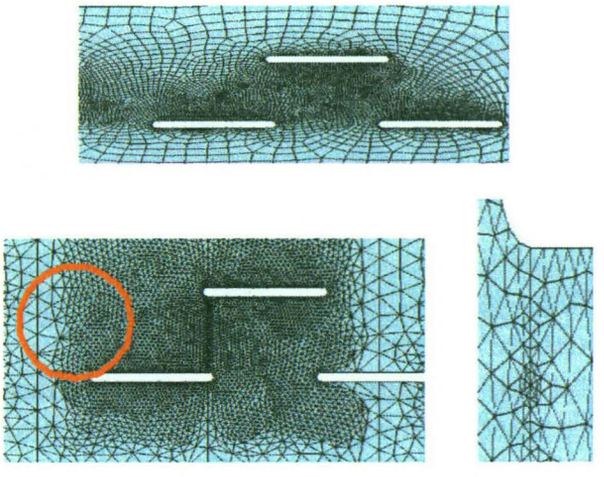

Figure 6 Discretization in the area and the cracks

4. The model of fracture by Burzynski hypothesis for brittle materials

Effort of material elements calculated according to the criterion Burzynski for brittle materials because it assumed a significant role in the tensile fatigue girder.

$$\sigma_{int} = \frac{\kappa+1}{2\kappa}\sqrt{(\sigma_x-\sigma_y)^2+(\sigma_y-\sigma_z)^2+(\sigma_x-\sigma_z)^2+6[\tau_{xy}^2+\tau_{yz}^2+\tau_{xz}^2]} + \frac{\kappa-1}{2}(\sigma_x+\sigma_y+\sigma_z) \tag{5}$$

where $\kappa = R_c/R_m$ (R_m – tensile strength and R_c – compressive strength).

Strain in ferrite was studied since its yield strength is quite low which affects the low resistance to fatigue of this fraction in the steel.

After carrying out numerical calculations corresponding to the load of forced displacement equal $\varepsilon_x = 0.075\%$ ($\cong$ g50 MPa) gave map stress reduced by hypothesis Burzynski. Then selects the item, in which the equivalent stresses reach a peak. This element is removed, a gap. We assume that after so many cycles to burst element which had maximum stress. This element is removed. Then repeat the calculations for the new arrangement of elements, and the next element is removed, followed by crack propagation is a method of lost items. After a series of calculations gave the crack path.

Metallographic examinations supplemented by numerical calculations and research mock–lamellar cracks allow analysis of their interaction in the pre–destruction and the process of cracking.

5. The process of cracking assuming a critical size factor K_{IC}

Structural design concepts traditionally use a strength-of-material approach for designing a component. This approach does not anticipate the elevated stress levels due to the existence of cracks. The presence of dry stresses stressful it can lead catastrophic failure of the structure.

Fracture mechanics accounts for the cracks or flaws in the structure. The fracture mechanics approach to the design of structures includes flaw size as one important variable, and fracture toughness replaces strength of the material as a relevant material parameter.

Fracture analysis is carried out using the stress intensity–factor criterion. When the stress–intensity–factor criterion is used, the critical value of the amplitude of the stress and deformation fields characterizes the fracture toughness.

The process of cracking lost can be analyzed by finite element models of fracture mechanics accepting. This method consists in the fact that when the apex slots intensity factor stress reaches a critical value, ie. $K_I = K_{IC}$ then it is assumed that elements in the top of the gap disappears, the gap is widening takes its propagation, a cycle calculation is repeated and again the rate is calculated stress intensity. In this way we get a line of crack propagation. In this case, using the finite element method (ANSYS program 14) assumes a special arrangement of the elements and homogeneous structure of the material. However, in fact, cracks are formed in non–uniform lamellar structure (i.e. pearlite + ferrite).

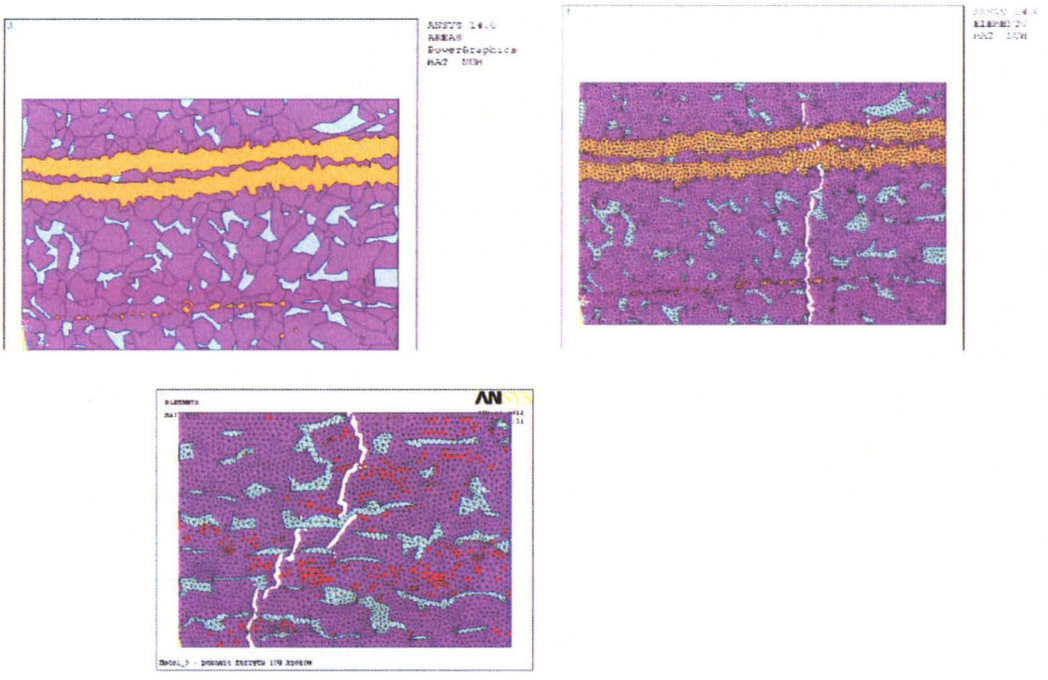

Figure 7 FEM models generated on the basis of metallographic

Figure 8 Details the sample taken for the calculation on the basis of metallographic

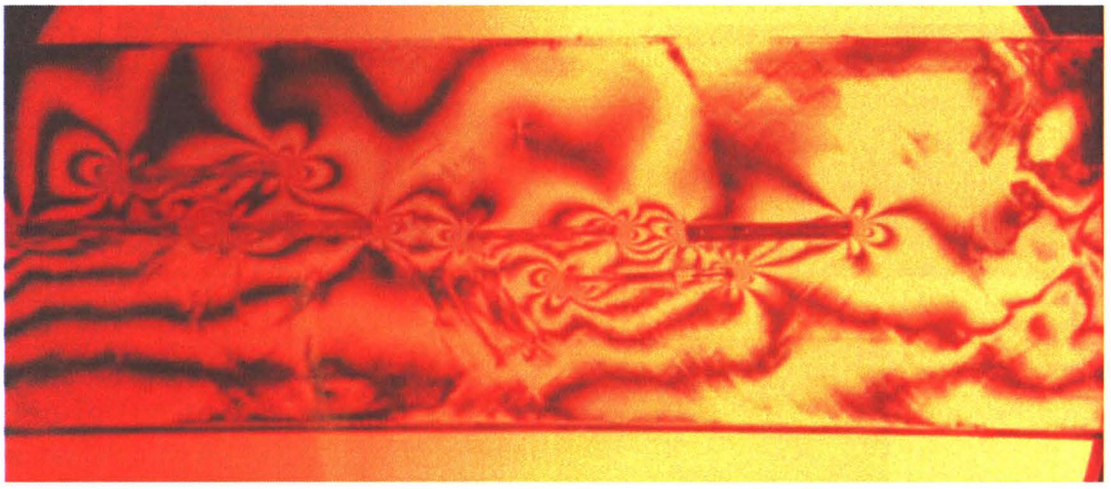

Figure 9 The results of the model tests. Isochromatic distribution in the model with non–metallic inclusions - isochromatic lines in the model photo elastic distribution isochromatic from destruction

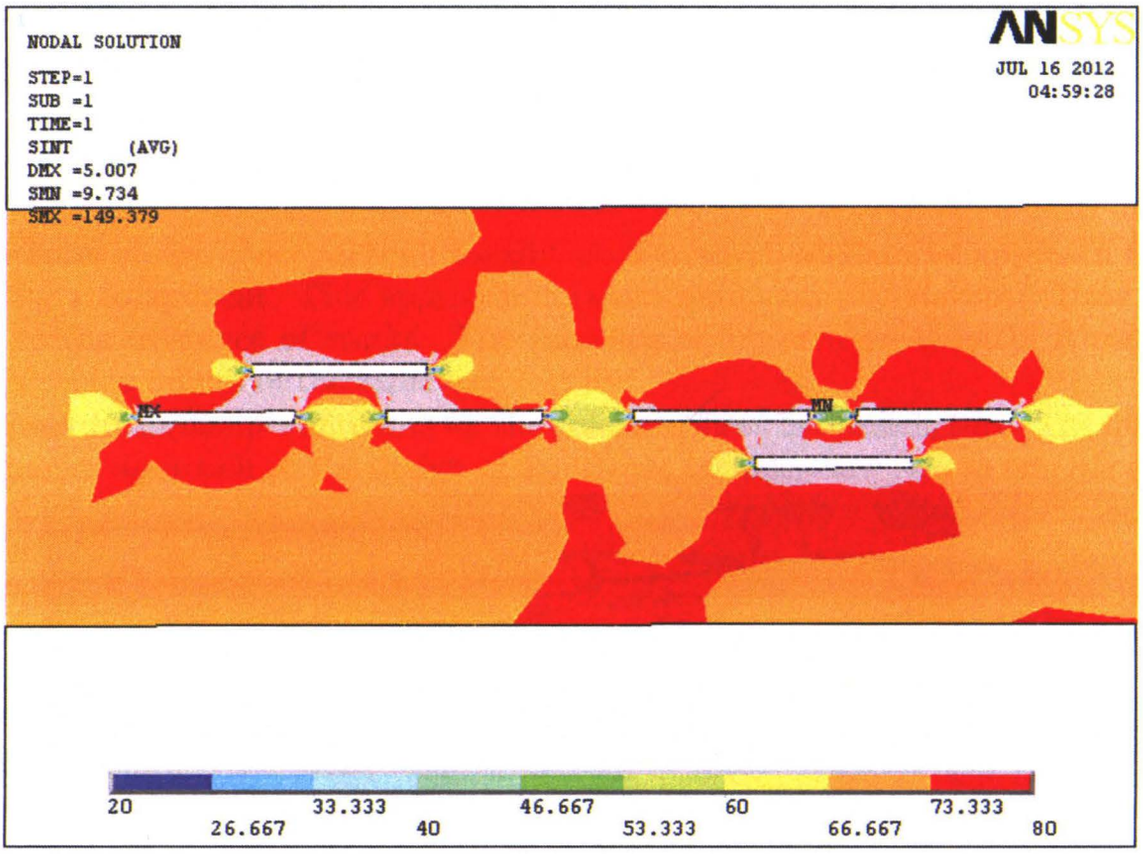

Figure 10 The results of numerical calculations. Izochrom distribution in the model with non–metallic inclusions in the model system photo elastic sample of the lamellar cracks

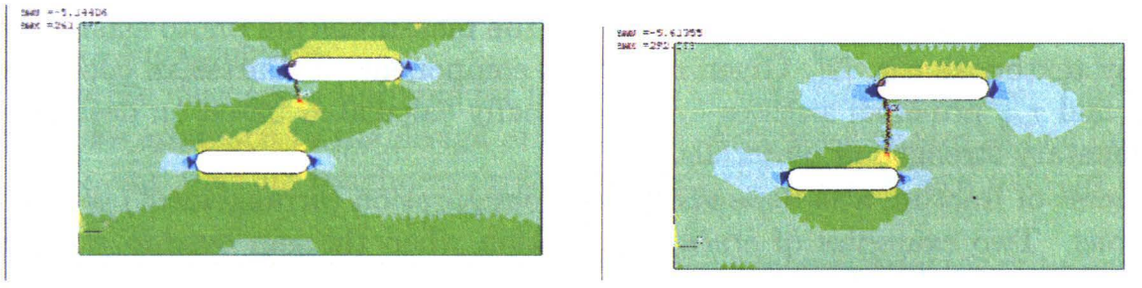

Figure 11 Numerical calculations cracking process. Beginning of cracking and larger cracks

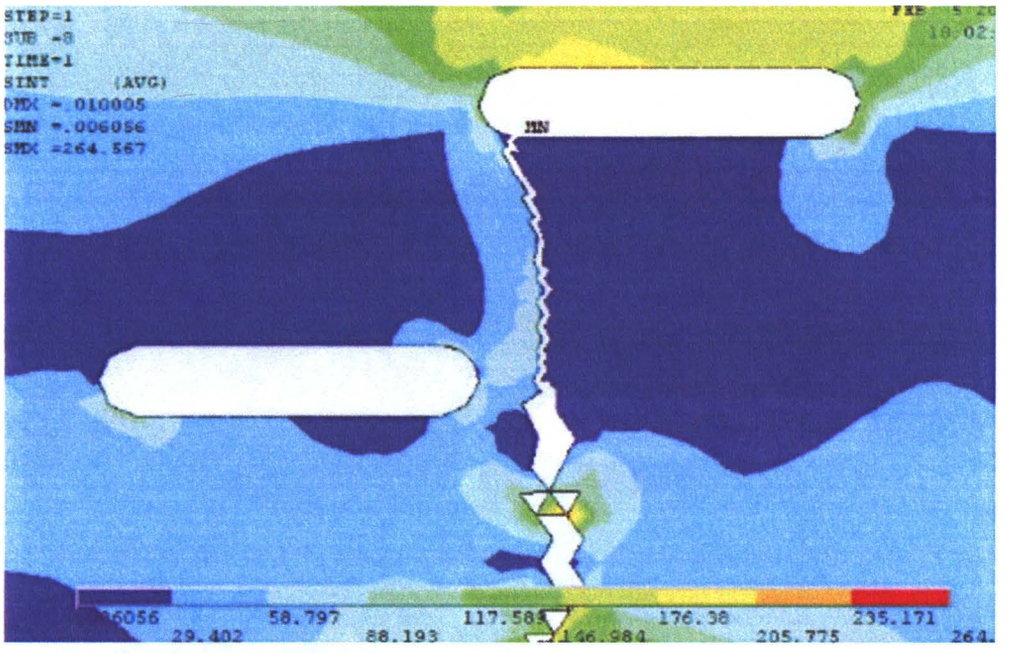

Figure 12 The results of numerical calculations – examples slits perpendicular to the non-metallic inclusions (lamellar) occurred during the tensile test

Non–metallic inclusions cause delamination of the structure, cracks perpendicular to the lamellar inclusions (slots) as well as along the stretching direction. There appears to changes in the distributions of the stresses which can give rise to shear stresses along the lines connecting the vertices of the inclusions.

Model tests and numerical calculations were also performed on photoelastic models with inclusions simulating non–metallic inclusions. Emptiness or cracks in optically active models allow the analysis of the stresses around cracks during stretching up to the phase of destruction.

Conduct research on photo elastic models (material optically active) allows you to perform tests in accordance with the theoretical assumptions as well as the guidelines, standards and enables further analysis of the stress in the whole area of the model.

Photo elastic study was carried out by increasing the load, and analyzed the state of stress (based on distributions of isochromatic) in order to determine the impact of voids on changes in the stress field and their mutual interaction in the environment voids or gaps.

General methods of procedure for taking the measurements photo elastic shown in many textbooks e.g. [2]. Given the stress components in Cartesian coordinates: σ_x, σ_y and τ_{xy} principal stresses - σ_1, σ_2 usually calculated based on designs used in elementary strength of materials.

Process of fracture also depends on the configuration (arrangement) of lamellar inclusions. Two examples of crack propagation when the gap overlap each other and they are slightly offset. In the first case fracture intersects both of cracks, in the second bypass the crack.

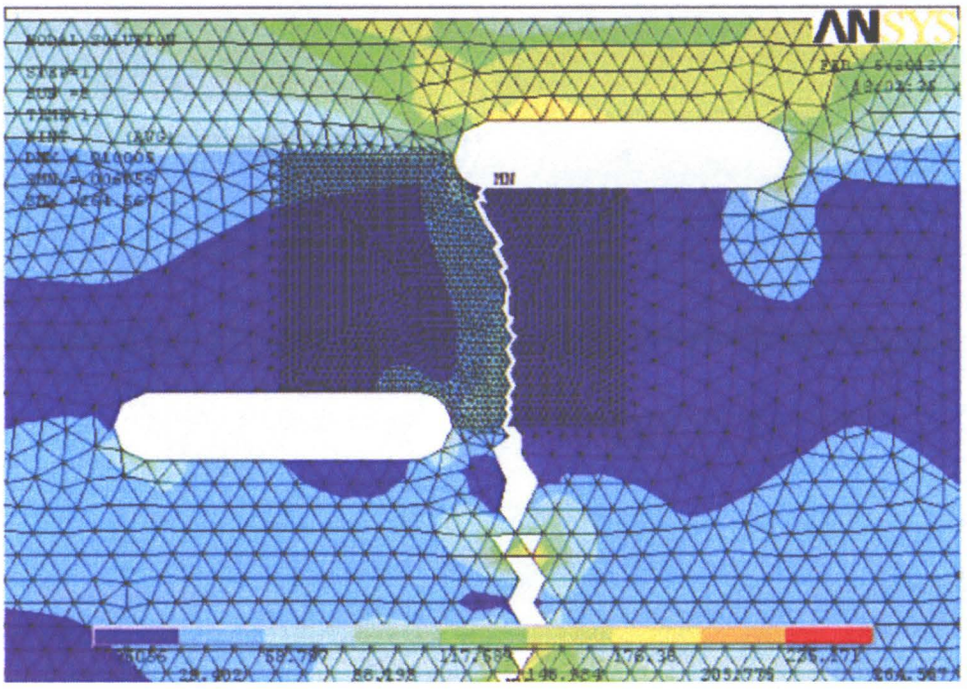

Figure 13 The results of numerical calculations – e.g. crack propagation if slots are slightly shifted

6. Conclusions

Non–metallic inclusions cause delamination of the structure, cracks perpendicular to the lamellar inclusions (slots) as well as along the stretching direction. occurs here changes in the distributions of the stresses which can give rise to shear stresses along the lines connecting the vertices of the inclusions. Embryos cracking are located near the apparent discontinuity structure. Initial cracks formed inside the sample rather than on their edges. The process of cracking test according to the hypothesis Burzynski consists in that the structure adopted by metallographic examination, in which the equivalent stresses reach a maximum is removed, a gap is generated. If you use the numeric lost element method (by ANSYS 14) assumes a special arrangement of the elements and homogeneous structure of the material and the model differs from the actual structure of the material.

Structural design concepts traditionally use a strength–of–material approach for designing a component. This approach does not anticipate the elevated stress levels

due to the existence of cracks. The presence of such stresses can lead to catastrophic failure of the structure.

Fracture mechanics accounts for the cracks or flaws in a structure. The fracture mechanics approach to the design of structures includes flaw size as one important variable, and fracture toughness replaces strength of material as a relevant material parameter.

Fracture analysis is carried out using the stress intensity-factor criterion. When the stress–intensity–factor criterion is used, the critical value of the amplitude of the stress and deformation fields characterizes the fracture toughness.

Under certain circumstances, the two criteria are equivalent.

References

[1] **Cherepanov, G. P.**: Mechanics of brittle fracture, *Mc Graw–Hill*, New York, **1979**.

[2] **Dyląg, Z., Jakubowicz, A. and Orloś, Z.**: Strength of Materials, (in Polish), Warsaw, *WNT*, **1996**.

[3] **Blum, A. and Niezgodziński T.**: Lamellar cracks, *Publisher Institute for Sustainable Technologies* – Monographs, (in Polish), **2007**.

[4] **Hutchinson, J. W.**: Plastic stress and strain fields at the crack tip, *J. Mech. Phys. Solids*, Vol. 16, 337–347, **1968**.

[5] **Neimitz, A.**: Fracture Mechanics, *PWN*, Warsaw, **1998**.

[6] **Seweryn, A.**: Numerical Methods in fracture mechanics, *Polish Academy of Sciences*, the Library of Applied Mechanics, IFTR Academy of Sciences, Warsaw, **2003**.

[7] **Sih, G. C.**: Hanbook of Stress–Intensity Factors, Bethlehem, *Leigh University Press*, Vol. 1, **1973**.

[8] **User's Guide 14 ANSYS**, ANSYS, Inc., Houston, USA.

[9] **Williams, M. L.**: On the Stress Distribution at the Base of a Stationary Crack, Trans. ASME, *Journal of Appl. Mechanics*, 3, pp. 109–114, **1957**.

[10] **Wu, E. M.**: Application of Fracture Mechanics is Anisotropic Plates, Trans. ASME, *Journal of Appl. Mechanics*, E, 34, pp. 967–974, **1967**.

[11] **Zienkiewicz, O. C.**: The Finite Element Method in Engineering Science, *Mc Graw–Hill*, London, New York, **1971**.